NMR Evidence for Higher-Order Multipole Order Parameters in NpO_2

Y. Tokunaga,[1] D. Aoki,[2] Y. Homma,[2] S. Kambe,[1] H. Sakai,[1] S. Ikeda,[1] T. Fujimoto,[1] R. E. Walstedt,[1] H. Yasuoka,[1] E. Yamamoto,[1] A. Nakamura,[1] and Y. Shiokawa[1,2]

[1]*ASRC, Japan Atomic Energy Agency, Tokai, Ibaraki 319-1195, Japan*

[2]*IMR Tohoku University, 2145-2 Narita Oarai Higashiibaraki Ibaraki 311-1313, Japan*

(Received 26 May 2006; published 19 December 2006)

We report a microscopic investigation of multipolar order parameters in the ordered state of NpO_2 conducted via ^{17}O NMR on a single crystal. From the angular dependence of hyperfine fields at ^{17}O nuclei, we have obtained clear evidence for the appearance of field-induced antiferro-octupolar as well as field-induced antiferro-dipolar moments below $T_0 = 26$ K. We have also observed oscillatory spin-echo decay, which is well understood in terms of small electric field gradients created by antiferro-quadrupolar ordering. This reveals that the quadrupolar order parameter is directly observable by means of NMR. The present NMR studies provide definitive support for a proposed longitudinal triple-q type octupolar-quadrupolar ordering model for NpO_2.

DOI: 10.1103/PhysRevLett.97.257601 PACS numbers: 76.60.−k, 75.25.+z

Multipolar degrees of freedom characteristic of f electrons bring rich and complex physics to rare-earth and actinide compounds. A number of unusual properties of f-electron systems have been discussed on the basis of underlying electric quadrupolar ordering. Furthermore, spontaneous ordering of magnetic octupolar moments has been proposed recently as a ''hidden'' order parameter in compounds such as $Ce_{1-x}La_xB_6$ [1–3], $SmRu_4P_{12}$ [4], URu_2Si_2 [5], and NpO_2 [6]. The low-temperature phase transitions in these compounds are suggested to break time reversal invariance without long-range magnetic dipolar order.

Compared with dipolar ordering, however, multipolar order parameters are difficult to investigate by conventional means. Although there are several indirect methods, recent identification of multipole order parameters can be credited mostly to resonant x-ray scattering (RXS) or neutron scattering; the former method directly probes the anisotropy of the f-electron shell and the latter probes field-induced antiferro-dipolar (FI-AFM) moments arising from multipoles. In the present work, however, we demonstrate that microscopic investigation of multipole order parameters is also possible by means of NMR through the hyperfine (HF) interactions. Our NMR results clearly demonstrate the occurrence of field-induced antiferro-octupolar (FI-AFO) as well as FI-AFM moments in the ordered state of NpO_2. Furthermore, we report oscillatory spin-echo decay behavior ascribed to a small electric field gradient (EFG) created by the antiferro-quadrupolar (AFQ) ordering. To our knowledge, this is the first example of f-electron quadrupolar order detection through quadrupolar interactions with ligand nuclei.

The phase transition in NpO_2 was originally discovered with specific heat measurements more than half a century ago [7], where the specific heat was found to exhibit a clear λ-type anomaly at $T_0 = 26$ K. However, neither long-range magnetic dipole order [8,9] nor internal lattice distortions [10,11] have been observed in this system below T_0. Instead, RXS measurements have been reported which suggest the occurrence of longitudinal, triple-$\mathbf{q}$ Γ_5 AFQ structure in the ordered state [12]. Moreover, the AFQ order has been proposed to be a *secondary* order parameter in a transition driven by *primary* Γ_5 antiferro-octupolar (AFO) order [6,12], since the AFQ order alone can not successfully explain the breaking of time reversal symmetry suggested by susceptibility [13] and μSR [14] measurements. The longitudinal triple-$\mathbf{q}$ Γ_5 AFO ordered ground state has also been corroborated by recent microscopic calculations based on the j-j coupling scheme [15,16]. Up to now, however, no direct evidence for a triple-$\vec{q}$ AFO structure has been obtained.

In a previous Letter, we have reported the results of the first ^{17}O NMR measurements on this system using a powder sample [17]. In the latter study, the observation of two inequivalent oxygen sites has confirmed the symmetry lowering associated with the *longitudinal* triple-$\mathbf{q}$ type ordering for $T < T_0$. We also noted the appearance of HF interactions associated with field-induced multipole moments in the ordered state. At that time, however, we could not resolve multiple HF components individually from the rather broad powder NMR spectra. In this Letter, we report a more detailed ^{17}O NMR study performed on a single crystal. The field-angle resolved NMR measurements provide definitive support for the proposed longitudinal triple-q AFO-AFQ ordering model for NpO_2.

A single crystal of 85 at.% ^{17}O enriched NpO_2 was grown by the chemical transport method. X-ray diffraction patterns confirmed a single-phase, cubic fluorite NpO_2 structure for the crystal. The ^{17}O NMR measurements were carried out using a superconducting magnet and a phase coherent, pulsed spectrometer. The field-angle dependence of the ^{17}O spectra was measured by means of a two-axis sample rotator installed in the experimental cryostat.

Figure 1 shows the temperature dependence of fast Fourier-transform (FFT) spectra obtained with magnetic field along the (a) $\langle 111 \rangle$ and (b) $\langle 100 \rangle$ axes of the crystal,

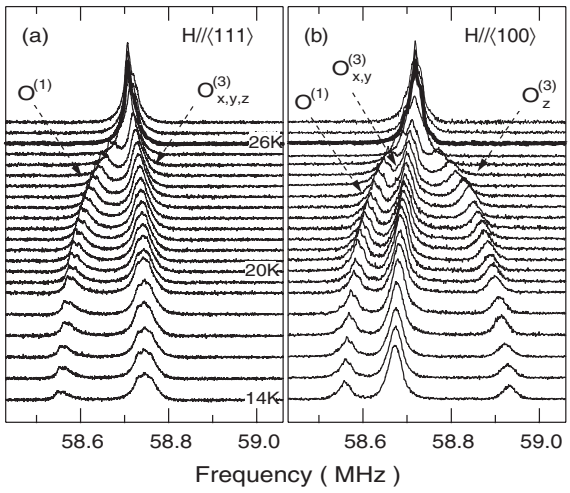

FIG. 1. FFT ^{17}O NMR spectra at a series of temperatures T below 27 K, with the $H = 10.17$ T magnetic field applied along the (a) ⟨111⟩ and (b) ⟨100⟩ directions of the crystal, respectively.

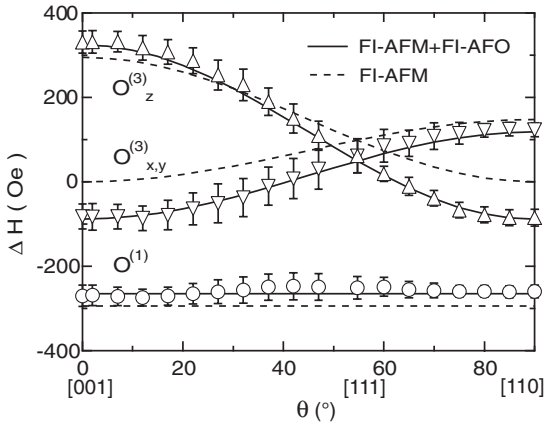

FIG. 2. The θ dependence of the NMR line splitting. The solid and dashed lines are model fits to the data (see text). These data were taken at $T = 17$ K and $H = 10.17$ T. The error bars indicate the half-width of the NMR peaks.

respectively. In the paramagnetic state above T_0, we have obtained a narrow, nearly symmetric spectrum. There is no quadrupole splitting, reflecting the cubic point symmetry at the O sites. In the ordered state, on the other hand, the spectrum gradually splits into several peaks, e.g., two peaks with $H \parallel \langle 111 \rangle$ and three peaks with $H \parallel \langle 100 \rangle$, revealing the occurrence of inequivalent oxygen sites associated with the lowering of site symmetry in the ordered state.

In the paramagnetic state, all the oxygen ions occupy equivalent positions (the 8c position) in the fluorite structure with the cubic space group (SG) $Fm\bar{3}m$. However, if *longitudinal* triple-**q** order is realized, the symmetry is lowered from $Fm\bar{3}m$ to $Pn\bar{3}m$ SG without any structural distortion [11,12]. This $Pn\bar{3}m$ SG has two inequivalent O sites (cubic: 2a and tetragonal: 6d) in a ratio of one to three, in agreement with our previous findings [17]. We denote the cubic site the $O^{(1)}$ site and the tetragonal sites the $O^{(3)}$ sites, respectively. In a single crystal, the $O^{(3)}$ sites are divided further into three inequivalent sites in a magnetic field, since their local symmetry is axial. We label them as $O_x^{(3)}$, $O_y^{(3)}$, and $O_z^{(3)}$, where their local symmetry axes are along the cubic crystal axes x, y, and z, respectively.

Figure 2 shows the angular dependence of the NMR line splitting $\Delta H = (f_{\rm res} - f_0)/\gamma$ in the ordered state, which illustrates the angular variation of HF fields at ^{17}O nuclei. Here $f_{\rm res}$ is the center of gravity of one of the observed NMR peaks, $f_0 = \gamma$H and $\gamma = 5.7719$ MHz/T for ^{17}O. θ is the polar angle of **H** relative to [001]. **H** rotates through the [111] to the [110] axis of the crystal. The applied field is thus given by $\mathbf{H} = (H_x, H_y, H_z) = \frac{H}{\sqrt{2}} \times (\sin\theta, \sin\theta, \sqrt{2}\cos\theta)$. In this rotation plane, the $O_x^{(3)}$ and $O_y^{(3)}$ sites are always equivalent. Therefore, the three curves in Fig. 2 correspond to the $O^{(1)}$, $O_z^{(3)}$, and $O_{x,y}^{(3)}$ sites, respectively. The nearly flat curve for the $O^{(1)}$ site corresponds to the isotropic nature of its HF field. On the other hand, other two curves for the $O_z^{(3)}$ and $O_{x,y}^{(3)}$ sites show a strong θ dependence due to the anisotropic nature of their HF fields. Although only the data at $H = 10.17$ T are shown in the figure, these NMR shifts are proportional to H.

The interpretation of the data in Fig. 2 is based on the proposed longitudinal triple-**q** Γ_5 AFO primary and AFQ secondary order parameters for NpO_2 [12,15,16]. The HF fields at the ^{17}O sites are derived from FI-AFM and FI-AFO moments arising from the secondary AFQ order [18]. The invariant form of the HF field contributions from these multipole moments, which are shown in Table I, has been derived by Sakai *et al.* using the method of symmetrized molecular orbital theory [19]. It is found that (1) the HF fields from the AFO moments all vanish by symmetry ($C_{1,1}$ terms in Table I), and (2) the FI-AFM and FI-AFO produce isotropic ($O^{(1)}$) and anisotropic ($O_{x,y,z}^{(3)}$) induced HF fields ($C_{1,1}$, $C_{1,3}$, and $C_{1,4}$ terms).

The HF fields shown in Table I produce NMR shift fields $\Delta H(\theta)$ proportional to their projection onto the applied field, i.e., onto the unit vector $((\sin\theta/\sqrt{2}, \sin\theta/\sqrt{2}, \cos\theta)$. The expected shift behavior from the $C_{1,2}$ term (FI-AFM) is then written $\Delta H_J^{(1)} = 2C_{1,2}H$, $\Delta H_J^{(3z)} = -2C_{1,2}H\cos^2\theta$, and $\Delta H_J^{(3xy)} = -C_{1,2}H\sin^2\theta$ for the $O^{(1)}$, $O_z^{(3)}$, and $O_{x,y}^{(3)}$ sites, respectively. In the same manner, the shift behaviors from the $C_{1,3}$ and $C_{1,4}$ terms (FI-AFO: T^β and T_{xyz} terms) are written $\Delta H_{T^\beta}^{(1)} = 0$, $\Delta H_{T^\beta}^{(3z)} = -2C_{1,3}H\sin^2\theta$, and $\Delta H_{T^\beta}^{(3xy)} = -C_{1,3}H(\cos^2\theta + 1)$ for T^β, and $\Delta H_{T_{xyz}}^{(1)} = C_{1,4}H$, $\Delta H_{T_{xyz}}^{(3z)} = -C_{1,4}H(1 - 2\cos^2\theta)$, and $\Delta H_{T_{xyz}}^{(3xy)} = -C_{1,4}H\cos^2\theta$ for T_{xyz}. As shown by solid lines in Fig. 2, we have found that the experimental results are well reproduced by taking $\Delta H(\theta) = \Delta H_J + \Delta H_{T^\beta} + \Delta H_{T_{xyz}}$ with $C_{1,2}H = -147.3$ Oe and $C_{1,3}H = C_{1,4}H = 29.5$ Oe for all three lines at $H = 10.17$ T [20]. This excellent agreement obtained with just three scaling parameters

TABLE I. The possible HF interactions at O nuclei in the longitudinal triple-**q** AFO-AFQ ordering state [19]. The definitions of coupling constants (c.c.) are given in Ref. [19]. $\mathbf{q_z}$ is the principal axis of the EFG tensor.

	$\mathbf{H} = \mathbf{0}$		$\mathbf{H} = (H_x, H_y, H_z)$		
Multipole	AFO	AFQ	FI-AFM	FI-AFQ	FI-AFO (T^β/T_{xyz})
c.c.	$C_{1,1}$	$C_{2,2}$	$2C_{1,2}$	$C_{2,5}$	$-2C_{1,3}/C_{1,4}$
$O^{(1)}$	0	0	(H_x, H_y, H_z)	0	$(0, 0, 0)/(H_x, H_y, H_z)$
$O_z^{(3)}$	0	$\mathbf{q_z} \parallel [001]$	$(0, 0, -H_z)$	$[O_{yz}H_x + O_{zx}H_y]$	$(H_x, H_y, 0)/(-H_x, -H_y, H_z)$
$O_y^{(3)}$	0	$\mathbf{q_z} \parallel [010]$	$(0, -H_y, 0)$	$[O_{xy}H_z + O_{yz}H_x]$	$(H_x, 0, H_z)/(-H_x, H_y, -H_z)$
$O_x^{(3)}$	0	$\mathbf{q_z} \parallel [100]$	$(-H_x, 0, 0)$	$[O_{zx}H_y + O_{xy}H_z]$	$(0, H_y, H_z)/(H_x, -H_y, -H_z)$

provides considerable support for the proposed longitudinal triple-**q** AFO-AFQ model for NpO_2. Note that, if the FI-AFO contributions ($\Delta H_{T^\beta} + \Delta H_{T_{xyz}}$) are omitted in the analysis, the resulting expressions fit the data very poorly, as shown by the dotted lines in Fig. 2. The contributions from the FI-AFO are therefore certainly required. To our knowledge, the only other case for which FI-AFO HF effects have been reported was for the AFQ ordered state of CeB_6 [21,22].

The scaling parameters $C_{1,2}$ are related to the FI-AFM moment J_{AF} and the coupling constant A_0 between ^{17}O nuclei and the FI-AFM moments, where $2C_{1,2}H \cong A_0 J_{\mathrm{AF}}$. If we adopt $|A_0| = |A_D| = 4.2$ kOe/μ_B estimated from the dipole calculation for NpO_2 [17], we obtain $J_{\mathrm{AF}} \sim 0.07\mu_B$/Np at $H = 10$ T. This value, however, should be regarded as an upper limit, since, in general, an enhancement of the HF coupling constant $A_0 > A_D$ is expected due to hybridization effects, etc. We can also expect that $J_{\mathrm{AF}} \gg J_{\mathrm{AFO}}$, since we also have $C_{1,3} = C_{1,4} = -\frac{1}{5}C_{1,2}$. Still, NMR is sensitive enough to resolve the contributions arising from these minuscule multipole moments at the microscopic level.

Next we discuss electric quadrupole effects. Table I shows both zero-field and field-induced effects ($C_{2,2}$, and $C_{2,5}$, respectively). The latter have not been observed up to now. We have found that the EFG generated by the zero-field term can be measured through the oscillatory spin-echo decay effects which it produces. Figures 3(a) and 3(b) show examples of such spin-echo oscillations and the corresponding FFT spectrum, where $M(\tau)$ is the integrated spin-echo intensity recorded as a function of the time τ between the excitation pulse and the refocusing pulse. The FFT spectrum shows a distinct peak at an oscillation frequency $\nu_m \simeq 5.2$ kHz. There are also harmonic satellite peaks around $2\nu_m$ and $3\nu_m$ positions. The oscillation behaviors are observed only at the $O^{(3)}$ sites, while $M(\tau)$ at the cubic $O^{(1)}$ site showed only a simple Gaussian decay.

The spin-echo oscillations are well understood in terms of an axially symmetric EFG at the $O^{(3)}$ sites. The first-order quadrupole splitting $a(\theta')$ causes spin-echo oscillations with a frequency $\nu_m = a/2\pi$. For $I = 5/2$ nuclei, oscillations of echo amplitude $M(\tau)$ (decay envelope suppressed) are given by the equation [23],

$$M(\tau) = m_0 + m_1\cos[a(\theta')\tau - \delta_1] + m_2\cos[2a(\theta')\tau - \delta_2] + m_3\cos[3a(\theta')\tau - \delta_3] + m_4\cos[4a(\theta')\tau - \delta_4],$$

where $a(\theta')/2\pi = \nu_Q(3\cos^2\theta' - 1)/2$, ν_Q is the electric quadrupole frequency, and θ' is the angle between **H** and the principal axis of the EFG tensor. The coefficients m_i and δ_i are determined by excitation pulse conditions. The equation shows echo oscillations at the primary frequency $\nu_m = a/2\pi$, with higher harmonic terms as well.

In general, the EFG at a nuclear spin is composed of lattice and electronic contributions. In the present case, however, the EFG is dominated by the electronic contributions, since the phase transition is not accompanied by any structural distortions [10,11]. The principal axis of the EFG can be determined from the angular dependence of ν_m, as shown in Fig. 3(c). By fitting the data to $\nu_m = \nu_Q(3\cos^2\theta' - 1)/2$, we identify the z axis as principal axis for the $O_z^{(3)}$ site, with the x or y axes for the $O_{x,y}^{(3)}$ sites. These

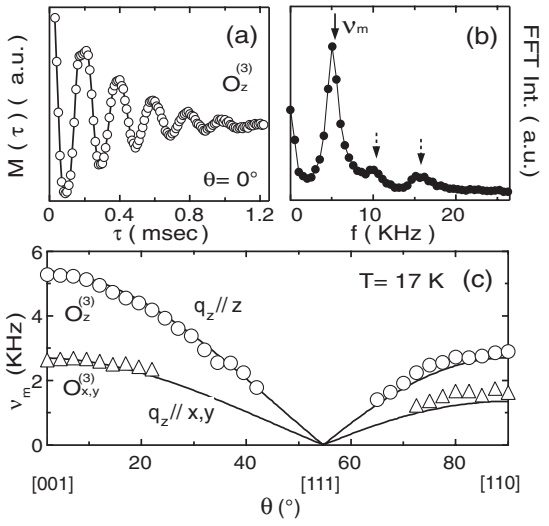

FIG. 3. Examples of (a) the spin-echo oscillations and (b) the corresponding FFT spectrum. (c) The field-angle dependence of ν_m. The solid curves are calculated on the assumption that the principal axes are along the z axis for the $O_z^{(3)}$ site and along the x or y axes for the $O_{x,y}^{(3)}$ sites, respectively. Note that $\mathbf{H} \parallel [111]$ makes the magic angle ($\theta' = 54.7°$) with these cubic axes. All data were taken at $T = 17$ K and $H = 10.17$ T.

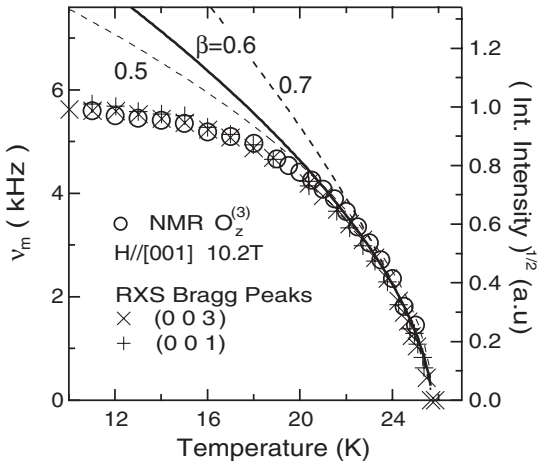

FIG. 4. The temperature dependence of ν_m at the $O_z^{(3)}$ site with $\mathbf{H} \parallel [001]$, plotted with the square root of the (001) and (003) Bragg peaks intensities reported for RXS studies [11,24]. The solid and broken lines are fits to power laws with critical exponents $\beta = 0.6 \pm 0.1$.

findings are in good accord with the $C_{2,2}$ terms for all four sites.

In a magnetic field, we can also expect the occurrence of FI-AFQ moments, as shown in Table I ($C_{2,5}$ terms). The confirmation of these FI-AFQ moments could be quite important, since they are induced directly from the primary AFO order. However, up to now we have not succeeded in detecting such a field-dependent EFG contribution, suggesting that more detailed NMR studies over a wide range of fields will be required.

The temperature dependence of ν_m, corresponding to the temperature dependence of the AFQ order parameter [19], is shown in Fig. 4. A nonzero ν_m rises up below T_0 and reaches a value $\nu_m \sim 5.7$ kHz at low temperatures. In the same figure, we also plot the square root of the (001) and (003) Bragg-peak intensities reported from RXS measurements [11,24]. These Bragg peaks were initially suggested to be of magnetic origin. However, they are now regarded as signaling the development of the AFQ order parameter. As seen in the figure, ν_m and the square root of the Bragg intensities follow a single curve below T_0. This confirms that both quantities reflect the same order parameter in NpO_2. The lines in the figure show fits to power laws with critical exponents $\beta = 0.6 \pm 0.1$. The large value of the critical exponent suggests a secondary character for the AFQ order in NpO_2 [24]. Note that the NMR data were taken at $H = 10$ T, while the RXS data were taken in zero field. Therefore, Fig. 4 also reveals that the critical exponents, as well as the transition temperature, are not measurably affected by an applied field, at least up to $H = 10$ T.

In conclusion, ^{17}O NMR has been successfully employed to probe the multipolar order parameters in the ordered state of NpO_2. We have used invariant forms for multipolar-induced HF fields from the literature to interpret the orientational dependence of ^{17}O NMR shifts. In this way, we have obtained clear evidence for the appearance of FI-AFO as well as FI-AFM moments below $T_0 = 26$ K. From the analysis, the magnitude of the FI-AFM is estimated to be $\sim 0.07 \mu_B$/Np at $H = 10$ T, and the HF field from the FI-AFO is to be a fifth part of that from the FI-AFM. In the ordered state, we have also observed spin-echo oscillations, which have been interpreted as axially symmetric EFG tensors created by the AFQ ordering. Using spin-echo oscillation frequencies, we have extracted the temperature dependence of the AFQ order parameter, which is in excellent agreement with the results from RXS measurements. Although direct evidence for the primary AFO order parameter has not succeeded yet, the present NMR results provide definitive support for the proposed longitudinal triple-q AFO-AFQ model for NpO_2.

The authors would like to thank K. Kubo, T. Hotta, R. Shiina, and O. Sakai for valuable discussions. This work was partly supported by a Grant for Basic Science Research Projects from the Sumitomo Foundation.

[1] Y. Kuramoto and H. Kusunose, J. Phys. Soc. Jpn. **69**, 671 (2000).
[2] H. Kusunose and Y. Kuramoto, J. Phys. Soc. Jpn. **70**, 1751 (2001).
[3] K. Kubo and Y. Kuramoto, J. Phys. Soc. Jpn. **73**, 216 (2004).
[4] M. Yoshizawa *et al.*, J. Phys. Soc. Jpn. **74**, 2141 (2005).
[5] A. Kiss and P. Fazekas, Phys. Rev. B **71**, 054415 (2005).
[6] P. Santini and G. Amoretti, Phys. Rev. Lett. **85**, 2188 (2000).
[7] D. W. Osborne *et al.*, J. Chem. Phys. **21**, 1884 (1953).
[8] R. Caciuffo *et al.*, Solid State Commun. **64**, 149 (1987).
[9] J. M. Friedt *et al.*, Phys. Rev. B **32**, 257 (1985).
[10] A. Boeuf *et al.*, Phys. Status Solidi A **79**, K1 (1983).
[11] D. Mannix *et al.*, Phys. Rev. B **60**, 15 187 (1999).
[12] J. A. Paixão *et al.*, Phys. Rev. Lett. **89**, 187202 (2002).
[13] P. Erdös *et al.*, Physica B+C (Amsterdam) **102**, 164 (1980).
[14] W. Kopmann *et al.*, J. Alloys Compd. **271**, 463 (1998).
[15] K. Kubo and T. Hotta, Phys. Rev. B **71**, 140404(R) (2005).
[16] K. Kubo and T. Hotta, Phys. Rev. B **72**, 132411 (2005).
[17] Y. Tokunaga *et al.*, Phys. Rev. Lett. **94**, 137209 (2005).
[18] O. Sakai *et al.*, J. Phys. Soc. Jpn. **72**, 1534 (2003).
[19] O. Sakai *et al.*, J. Phys. Soc. Jpn. **74**, 457 (2005).
[20] In the analysis, we assumed that there is no isotropic background shift below T_0. This assumption is supported by the very small shift found in the paramagnetic state. The tetrahedral symmetry around an O ion cancels the dipolar contribution from uniform magnetization [17].
[21] O. Sakai *et al.*, J. Phys. Soc. Jpn. **66**, 3005 (1997).
[22] M. Takigawa *et al.*, J. Phys. Soc. Jpn. **52**, 728 (1983).
[23] H. Abe *et al.*, J. Phys. Soc. Jpn. **21**, 77 (1966).
[24] R. Caciuffo *et al.*, J. Phys. Condens. Matter **15**, S2287 (2003).